Analysis of the Acceleration Characteristics of Manipulators

Alan Bowling and Oussama Khatib

Robotics Laboratory
Department of Computer Science, Stanford University
Stanford, CA 94305, USA

Abstract

Characterizing the acceleration properties at the end effector is crucial for the analysis, design, and control of robot manipulators. In previous efforts aimed at addressing this problem, the end-effector acceleration has been treated as a vector combining both the linear and angular accelerations. The methodology presented in this article provides characterizations of these two different types of accelerations and describes the relationship between them. This work is a extension of our previous studies on manipulator inertial and acceleration properties. The treatment relies on the *ellipsoid expansion* model, a simple geometric approach to efficiently analyze end-effector accelerations. Results of the application of this analysis to the PUMA 560 manipulator are discussed.

1 Introduction

The end-effector acceleration is an important measure of the dynamic performance of a manipulator. Yoshikawa [1] proposed the dynamic manipulability ellipsoid (DME) to characterize this acceleration. In order to deal with the differences between linear and angular accelerations, Yoshikawa used scaling factors to bring their magnitudes into range with each other.

In another study, Khatib and Burdick [2] proposed the hyper-parallelepiped of acceleration for the description of the end-effector acceleration characteristics. Their hyper-parallelepiped is obtained from the torque/acceleration relationship, which maps the hyper-cube of normalized torque bounds into accelerations. Inscribing a hyper-sphere in the acceleration hyper-parallelepiped yields a measure of the isotropic acceleration. This acceleration has been defined as the largest magnitude of acceleration the end effector is capable of producing along or about any direction. Scaling factors were also used to deal with the differences between linear and angular accelerations. The mapping of torque bounds into end-effector accelerations has been also analyzed by Kim and Desa [3]. However, rotational motions were not treated in their study.

By their different natures, linear and angular accelerations are difficult to analyze as components of a single vector. The use of scaling to address this problem does not lessen the difficulty in practice. Scaling factors are indeed difficult to set and their selection is somewhat arbitrary. The approach presented in this article is based on the *ellipsoid expansion* model which provides separate characterizations of linear and angular accelerations in order to determine the relationship between them. The ellipsoid expansion model provides a simple geometric solution to the system of inequalities associated with the actuators bounds. This approach is used for the analysis of the acceleration characteristics of a PUMA 560 manipulator.

2 Problem Statement

The problem discussed here is to determine, for a given configuration, the simultaneously achievable isotropic linear and angular accelerations, given the bounds on the actuator torques. In this paper, the acceleration characteristics is studied at zero joint velocities. The derivation of the governing equation for this analysis begins with the operational space equations of motion. These equations describe the dynamics of the end effector with respect to linear and angular velocities,

$$\Lambda_0(\mathbf{q})\dot{\vartheta} + \mu_0(\mathbf{q}, \dot{\mathbf{q}}) + \mathbf{p}_0(\mathbf{q}) = \mathbf{F}_0; \tag{1}$$

where

$$\vartheta \triangleq \begin{bmatrix} \mathbf{v} \\ \omega \end{bmatrix} = J_0(\mathbf{q})\dot{\mathbf{q}}; \tag{2}$$

In equation (1), $\mathbf{q}$ is the vector of n joint coordinates, $\Lambda_0(\mathbf{q})$ is the kinetic energy matrix, $\mu_0(\mathbf{q}, \dot{\mathbf{q}})$ is the centrifugal and Coriolis force vector, $\mathbf{p}_0(\mathbf{q})$ is the gravity force vector, and $\mathbf{F}_0$ is the vector of forces and moments acting at the end-effector. In equation (2) $\mathbf{v}$ and ω are the end effector linear and angular velocities and $J_0(\mathbf{q})$ is the basic Jacobian. The joint torque vector τ corresponding to $\mathbf{F}_0$ is

$$\tau = J_0^T \mathbf{F}_0. \tag{3}$$

The bounds on τ can be written as

$$-\tau_{bound} \ \leq \ \tau \ \leq \ \tau_{bound}. \tag{4}$$

Using equations (1), (3), and (4), and setting $\dot{\mathbf{q}}$ to zero yields,

$$-\tau_{bound} \ \leq \ J_0^T \Lambda \dot{\vartheta} + J_0^T \mathbf{p}(\mathbf{q}) \ \leq \ \tau_{bound}. \tag{5}$$

To normalize the bounds on τ, we introduce the diagonal matrix N with components $N_{ii} = \frac{1}{\tau_{bound(i)}}$,

$$-\mathbf{1} \ \leq \ N J_0^T \Lambda \dot{\vartheta} + N J_0^T \mathbf{p}(\mathbf{q}) \ \leq \ \mathbf{1}; \tag{6}$$

where $\mathbf{1}$ is a vector with each element equal to one. The above equation can be rewritten as,

$$\tau_{lower} \ \leq \ [E_1 \ E_2] \begin{bmatrix} \dot{v} \\ \dot{\omega} \end{bmatrix} \ \leq \ \tau_{upper}; \tag{7}$$

where

$$[E_1 \ E_2] = N J_0^T \Lambda; \tag{8}$$

$$\tau_{upper} = \mathbf{1} - N J_0^T \mathbf{p}(\mathbf{q}); \tag{9}$$

$$\tau_{lower} = -\mathbf{1} - N J_0^T \mathbf{p}(\mathbf{q}). \tag{10}$$

Finally, the relationship between bounded torques and linear and angular accelerations is given by,

$$\boxed{\tau_{lower} \ \leq \overline{\tau} \leq \ \tau_{upper} \ ; \ \text{ with } \quad \overline{\tau} = E_1 \dot{\mathbf{v}} + E_2 \dot{\omega}} \tag{11}$$

The separation of the linear and angular acceleration in (11) is motivated by the need to analyze each of them independently.

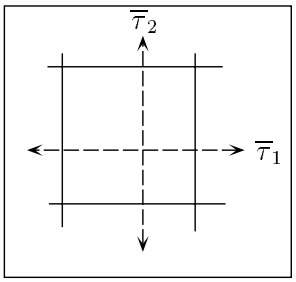

Figure 1: Bounds on $\overline{\tau}$

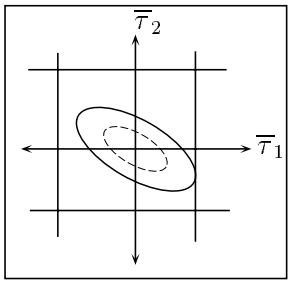

Figure 2: Ellipsoid for τ_v.

3 Ellipsoid Expansion Model

Our approach is to represent each vector in equation (11) as a geometric object. The bounds in equation (11) are represented as an n-dimensional hypercube, whose center is shifted from the origin by the gravity effect, i.e. $NJ_0^T\mathbf{p}(\mathbf{q})$. An example of simple 2-dimensional boundaries is shown in Figure 1. Any resultant vector, $\overline{\tau}$, that lies within the boundaries will satisfy the inequality. We now consider the case where, $\dot{\omega} = 0$, in the inequality of equation (11).

$$\tau_{lower} \;\leq\; \overline{\tau}_v \;\leq\; \tau_{upper} \;;\; \text{with} \quad \overline{\tau}_v = E_1\dot{\mathbf{v}}. \tag{12}$$

Geometrically, the isotropic linear acceleration can be represented as a sphere with some radius a, $\dot{\mathbf{v}}^T\dot{\mathbf{v}} = a^2$. The value of a represents the magnitude of the achievable linear acceleration in any direction, i.e the isotropic acceleration. This value (a) is determined by the bounds imposed on the actuator torques, described by equation (12). Consider the relationship between accelerations and torques,

$$\tau_v = E_1\dot{\mathbf{v}}.$$

With respect to $\dot{\mathbf{v}}$, the above relationship is an over constrained system of equations, whose unique solution is given by

$$\dot{\mathbf{v}} = E_1^+ \;\tau_{\mathbf{v}}; \tag{13}$$

where E_1^+ is the left inverse[1] of E_1. Using equation (13), the sphere of acceleration $\dot{\mathbf{v}}^T\dot{\mathbf{v}} = a^2$ is transformed into,

$${\tau_{\mathbf{v}}}^T(E_1E_1^T)^+\tau_{\mathbf{v}} = a^2. \tag{14}$$

E_1 is a full rank matrix. Its rank is three, two, or one, following the freedom of the end-effector for linear motions. Equation (14) represents therefore an ellipsoid of dimensions three or less, which lies in the n-dimensional space, as illustrated in Figure 3.

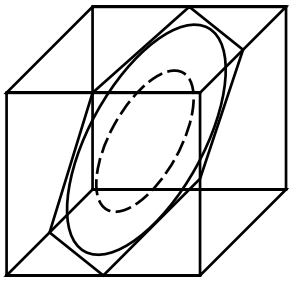

Figure 3: Ellipse Expansion in 3D.

Our procedure to determine the isotropic acceleration is based on expanding the ellipsoid (14) by changing a until it is tangent to one of the torque bounds. In Figure 2 this process is shown for a

[1] given by the left pseudo-inverse $E_1^+ = (E_1^T\;E_1)^{-1}\;E_1^T$.

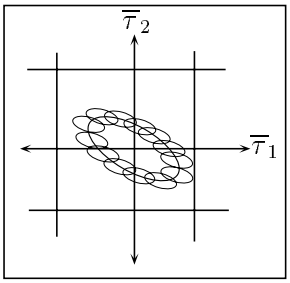

Figure 4: Ellipsoids Added.

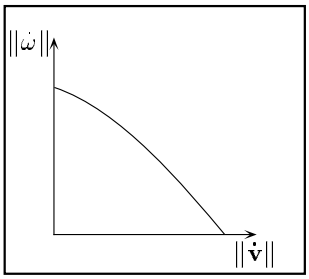

Figure 5: Isotropicity Curve.

very simple case. The dashed ellipse in the figure corresponds to $a = 1$. Note that only the vectors associated with the tangent points ($2n$ points on the $2n$ torque boundaries) need to be examined. Figure 3 illustrates an example of a three-dimensional torque space and where E_1 is of rank two. The dashed ellipse in this figure corresponds to $a = 1$.

Let us now consider the general case of equation (11) where $\dot{\omega} \neq 0$. Just as in the linear case, the isotropic angular acceleration is represented as a sphere with some radius, b, in acceleration space, $\dot{\omega}^T\dot{\omega} = b^2$. Similarly to the linear acceleration, this sphere can be transformed into torque space by solving for $\dot{\omega}$ in

$$\overline{\tau}_\omega = E_2\dot{\omega}.$$

This yields,

$$\begin{aligned} \overline{\tau}_v^T(E_1E_1^T)^+\overline{\tau}_v &= a^2 \\ \overline{\tau}_\omega^T(E_2E_2^T)^+\overline{\tau}_\omega &= b^2. \end{aligned} \tag{15}$$

To insure that the sum of the vectors $\overline{\tau}_v$ and $\overline{\tau}_\omega$ remains within the bounds, all possible combinations of these two vectors must be considered. This process is represented as a mapping of one ellipsoid onto every point on the surface of the other ellipsoid. This procedure is graphically illustrated in in Figure 4. In the general case, the resulting surface is a hollow ellipsoid shell. However, there is no need to determine an equation for this surface. It is only necessary to examine the vectors representing the tangency points between each ellipsoid and the bounding box. Corresponding vectors are added.

Changing the magnitudes of one or the other or both until the surface is tangent to a bound yields a multiplicity of solutions for a and b. The multiplicity of solutions for the isotropic linear and angular acceleration is represented by a curve, as shown in Figure 5. This curve provides a complete picture of the coupling between isotropic linear and angular accelerations at a given configuration. Currently, this curve is generated by finding specific points on the curve and joining them with line segments. These curves can be computed at different configurations in the workspace to obtain an overall picture of the isotropic accelerations for the workspace of the manipulator.

Information concerning how much the end-effector accelerations vary in different directions at a given configuration also can be obtained from this model as the condition numbers of the matrices E_1 and E_2. The condition numbers characterize the extent to which acceleration greater than the isotropic acceleration can be achieved in some directions. The larger the condition number is, the larger the difference in acceleration magnitude the system will have.

Other information from this analysis concerns the manipulator's actuators. For instance, the limiting actuator(s) can be determined simply by examining which boundary is most constraining to the ellipsoids; which boundary is reached first and most often. Depending on the manipulator, there is the possibility that increasing the most limiting actuator torque(s) will increase the isotropic accelerations.

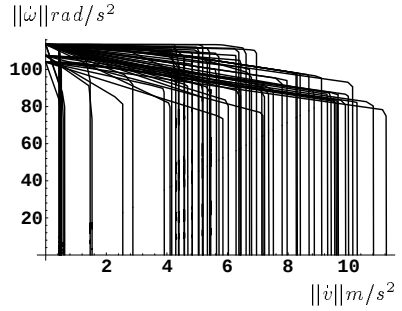

Figure 6:

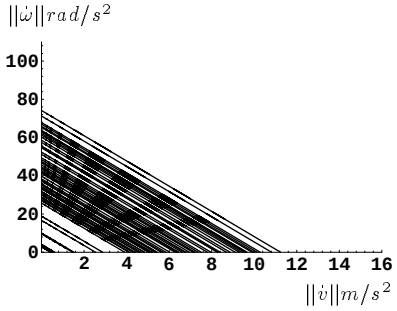

Figure 7:

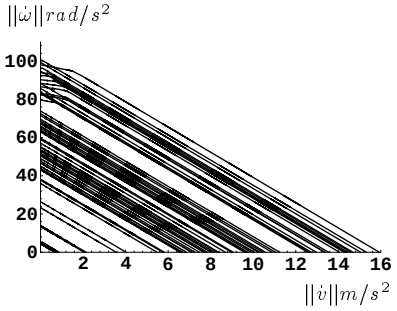

Figure 8:

4 Application to the PUMA 560

The approach presented above is illustrated here on the PUMA 560. The motor torque bounds are found by subtracting the breakaway torques from the maximum torques as given in [4];

$$\{\tau_1, \tau_2, \tau_3, \tau_4, \tau_5, \tau_6\}_{max} = \{1.45Nm, 1.70Nm, 1.62Nm, 0.30Nm, 0.27Nm, 0.26Nm\}$$

. Figures 6, 7, and 8 show the results of analysis of the PUMA 560 for different manipulator parameters. Each figure shows an overlay of the isotropicity curves calculated at 1056 different configurations in the workspace. For all of the configurations the wrist is in the same position in a well conditioned part of the wrist workspace. The 1056 configurations are generated by taking all possible combinations of the joint angle sets, shown in Table 1.

Table 1.

Joint Angle	Angle Set
$q1$	$0°, 30°, 60°, 90°, 120°, 150°, 180°, 210°, 240°, 270°, 300°, 330°$
$q2$	$45°, 15°, 0°, -30°, -60°, -90°, -120°, -150°, -180°, -210°, -225°$
$q3$	$-45°, -15°, 0°, 30°, 60°, 90°, 120°, 135°$
$\{q4, q5, q6\}$	$\{0°, 90°, 0°\}$

In Figure 6, the isotropicity curves for the wrist point of the PUMA 560 are shown. Note that the curve that is closest to the origin has a very small domain. This means that there are configurations in the test set which are near singularities. The shape of the curves indicates that linear and angular accelerations are nearly decoupled at the wrist point; Λ_0 is nearly block diagonal. An operational point where linear and angular accelerations are completely decoupled will have an isotropicity curve which forms a rectangle with the two coordinate axes. Figure 7 shows the isotropicity curves for an operational point 6 inches out from the wrist point. The curves show a large increase in the coupling between linear and angular accelerations as we move away from the wrist point. Overall both figures show that the isotropic accelerations vary quite a bit over the chosen configurations in the workspace. The main use of these curves is to specify the minimum guaranteed isotropic linear and angular acceleration for a particular operational point. However, such a specification will depend on a chosen operational envelope and the sampled configuration(s).

Another result from the analysis is that the actuator at joint 2 is the most constraining to the isotropic accelerations of Figure 7; this actuator bounds the ellipsoids most often. It is followed by the actuator of joint 1. Figure 8 results from increasing the maximum torques at joints 1 and 2 both by 40%. Comparing Figures 7 and 8 shows an increase in the isotropic accelerations in most cases.

The condition numbers of E_1 and E_2 for the two different operational points are shown in Figures 9 and 10. Each point represents the condition number of E_1, $\kappa(E_1)$, and E_2, $\kappa(E_2)$, at a particular configuration from the set of configurations of Table 1.

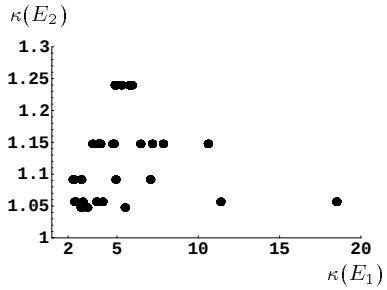

Figure 9: Condition of Wrist Point.

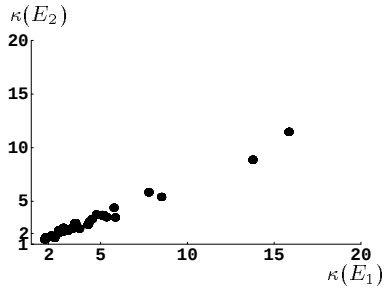

Figure 10: Condition of Oper. Point.

Figure 9 shows the condition numbers for the wrist point. Note that the angular acceleration is mostly isotropic. The largest and smallest condition numbers for the linear acceleration are, 58.5 and 2.3, and for the angular accelerations, 1.3 and 1.1.

Figure 10 represents the operational point six inches from the wrist point. The largest and smallest condition numbers for linear accelerations are 2.1 and 55.1 respectively. For angular accelerations they are 1.6 and 42.0.

5 Conclusion

We have presented an approach based on the *ellipsoid expansion* model for the analysis of linear and angular accelerations, given the limits on actuator torque capacities. This model has been shown to provide a simple geometric solution for determining these accelerations. The result of the analysis is an isotropicity curve which completely describes the dependency between the isotropic accelerations associated with linear and angular motions. Characterization of the workspace of a manipulator involves examining isotropicity curves at different configurations throughout the workspace. Condition numbers have been used to provide a measure of the extent of magnitude variations for the linear and angular accelerations in different directions. The results obtained with the PUMA 560 manipulator, illustrate the effectiveness of this approach for acceleration analysis. This approach is being extended for the optimization of acceleration properties in the design of manipulator systems.

References

[1] Yoshikawa T.; Dynamic Manipulability of Robot Manipulators. Proc. 1985 IEEE International Conference on Robotics and Automation, St. Louis, 1985, pp. 1033-1038.

[2] Khatib, O. and Burdick, J. "Dynamic Optimization in Manipulator Design: The Operational Space Formulation," *Robotics and Manufacturing Automation,* M. Donath and M. Leu, eds., *ASME Winter Annual Meeting,* Miami, 1985, PED-Vol. 15, pp. 169-174, (also available in The International Journal of Robotics and Automation, vol.2, no.2, 1987, pp. 90-98.)

[3] Kim, Y. and Desa, S.; *The Definition, Determination, and Characterization of Acceleration Sets for Spatial Manipulators*, The International Journal of Robotics Research, vol.12, no.6, pp. 572-587, December 1993.

[4] Armstrong, B., Khatib, O., and Burdick, J.; *The Explicit Model and Inertial Parameters of the PUMA 560 Arm*, Proceedings IEEE International Conference on Robotics and Automation, vol.1, pp. 510-518, 1986.